The Analysis of Proteasome Associated Protein, Ecm29

A Dissertation Submitted to

the Graduate School of Life and Environmental Sciences,

the University of Tsukuba

in Partial Fulfillment of the Requirements

for the Degree of Philosophy in Science

(Doctoral Program in Biological Science)

Kousuke HARATAKE

Table of Contents

Abstract ·····1

Abbreviations ·····2

General Introduction ·····4

Chapter 1: Phenotype of *KIAA0368* knockout mice

1.1 Summary ·····7

1.2 Introduction ·····8

1.3 Materials and Methods ·····9

1.4 Results ·····13

1.5 Discussion ·····16

Chapter 2: Regulation of proteasome under oxidative stress

2.1 Summary ·····17

2.2 Introduction ·····18

2.3 Materials and Methods ·····20

2.4 Results ·····23

2.5 Discussion ·····26

General Discussion ·····28

Acknowledgements ·····30

References ·····31

Tables ·····40

Figures ·····43

Abstract

Many cellular stresses cause damages of intracellular proteins, which are eventually degraded by the ubiquitin and proteasome system. The proteasome is a multicatalytic protease complex composed of 20S core particle and the proteasome activators that regulate the proteasome activity. Ecm29 is a 200 kDa protein encoded by *KIAA0368* gene, associates with the proteasome, but its role is largely unknown. Here *KIAA0368*-deficient mice were generated and I investigated the function of Ecm29 in stress response. *KIAA0368*-deficient mice showed normal peptidase activity and proteasome formation at normal condition. Under stressed condition, 26S proteasome dissociates in wild-type cells, but not in *KIAA0368*$^{-/-}$ cells. This response was correlated with efficient degradation of damaged proteins and resistance to oxidative stress of *KIAA0368*$^{-/-}$ cells. Thus, Ecm29 is involved in the dissociation process of 26S proteasome, providing a clue to analyze the mechanism of proteasomal degradation under various stress condition.

Abbreviations

ATP: Adenosine triphosphate

Blm10: Bleomycin resistant protein 10

CP: Core particle

DTA: Diphtheria toxin A

D-MEM: Dulbecco's modified Eagle's medium

DNP: 2,4-Dinitrophenol

DNPH: 2,4-Dinitrophenyl hydrazine

DTT: Dithiothreitol

Ecm29: Extracellular mutants 29

EDTA: ethylenediaminetetraacetic acid

ELISA: Enzyme-linked immunosorbent assay

H&E: Haematoxylin and eosin

HEAT: Huntingtin, elongation factor 3, protein phosphatase 2A and target of rapamycin 1 kinase

KO: Knockout

MEF: Mouse embryonic fibroblast

MHC: Major histocompatibility complex

PA: Proteasome activator

PAGE: Poly acrylamide gel electrophoresis

PBS: Phosphate buffered saline

PCR: Polymerase chain reaction

PFA: Paraformaldehyde

PMSF: Phenylmethylsulfonyl fluoride

RP: Regulatory particle

Rpn: Regulatory particle non-ATPase

Rpt: Regulatory particle ATPase

SDS: sodium dodecyl sulphate

Suc-LLVY-AMC: Succinyl-Leucine-Leucine-Valine-Tyrosine-7-amino-4-methylcoumarine

TBS-T: Tris-buffered saline-0.1% Tween 20

WCL: Whole cell lysate

WST: Water-soluble tetrazolium salts

WT: Wild-type

General Introduction

Intracellular protein degradation is essential for cell viability and regulates wide range of biological processes such as immune response, cell cycle, and DNA repair. Intracellular protein degradation is mainly carried out by two processes, the ubiquitin-proteasome system and autophagy (Hershko and Ciechanover, 1998, Mizushima and Komatsu, 2011). The ubiquitin-proteasome system is responsible for selective protein degradation. Ubiquitin molecules covalently tether the target proteins specifically by several hundreds of ubiquitin ligases. Ubiquitylated proteins are then recognized and subjected to degradation by proteasomes in an ATP dependent manner.

The proteasome is a multicatalytic protease complex that functions in eukaryotic intracellular protein degradation (Goldberg, 1990). The proteasome is composed of over 60 subunits, and the subunits can be divided into 2 particles, one is catalytic core particle (CP) and the other is proteasome activator. The CP is also called 20S proteasome. CP is a barrel shaped complex composed of four stacked rings. The rings are composed of two outer α rings and two inner β rings. Both of these two rings are composed of structurally resembled 7 subunits named α1-7 and β1-7 subunits (Groll et al., 1997). Protein degradations are carried out by β1, β2 and β5 subunits in the CP. Each of these subunits is responsible for different peptidase activity, β1 for caspase-like activity, β2 for trypsin-like activity and β5 for chymotrypsin-like activity (Heinemeyer et al., 2004). Unless proteasome activators do not bind to the CP, α rings are generally closed and substrates are unable to enter to the inner core of the CP where the substrates are degraded (Whitby et al., 2000, Groll et al., 1997, Kohler et al., 2001).

The proteasome activators bind to both ends of CP and regulate the proteasome activity.

Several kinds of proteasome activators were identified up to date, such as PA700 (also called 19S regulatory particle), PA28αβ hetero-heptamer, PA28γ homo-heptamer (also called 11S regulator or REG) and PA200 (Stadtmueller and Hill, 2011). 19S regulatory particle (RP) conjugated proteasome is called 26S proteasome and it fulfils degradation of ubiquitylated proteins. In ubiquitin-proteasome system, polyubiquitin chains are formed on the substrates and become a degradation signal for 26S proteasome (Hershko and Ciechanover, 1998). 19S RP has a role in the ubiquitin chain recognition, removal of ubiquitin chain from substrate and unfolding of the substrate (Deveraux et al., 1994, Lam et al., 2002, Finley, 2002). Binding of 19S RP to the CP requires ATP, but binding of other proteasome activators such as PA28 and PA200, does not. PA28αβ heterocomplex facilitates the antigen processing in MHC class I antigen presentation (Groettrup et al., 1996, Dick et al., 1996). PA28γ complex plays important roles in growth and proliferation according to the knockout mice phenotypes (Murata et al., 1999). The function of PA200 is linked to spermatogenesis and DNA repair, because *Psme4* (which encodes PA200) -deficient mice shows abnormalities in male reproduction and damaged DNA repair (Qian et al., 2013).

Extracellular mutants 29 (Ecm29), encoded by *KIAA0368* gene, was originally identified as a mutant defective in cell wall biogenesis by yeast mutant screening (Lussier et al., 1997). Further research revealed that Ecm29 interacts with 26S proteasome (Gavin et al., 2002). However the function of Ecm29 on proteasome activities and its physiological role in mammalian cells has been unknown.

In this study, I have aimed to elucidate the physiological role of Ecm29 and its role on proteasome activities. In chapter 1, I analyzed the phenotypes of *KIAA0368*-deficient mice. *KIAA0368*-deficient mice were apparently healthy and their proteasomal peptidase

activities were not impaired. In chapter 2, I investigated the regulation of proteasome under oxidative stress in *KIAA0368*-deficient cells. This investigation revealed impairment of proteasome regulation in *KIAA0368*-deficient cells.

Chapter 1

Phenotype of *KIAA0368* knockout mouse

1.1 Summary

Previous researches in yeast reported many features of Ecm29 on proteasome regulation such as facilitating the tethering between CP and 19S RP, destabilizing the binding of 26S proteasome and intracellular translocation of proteasome. However, its physiological importance and the regulation of proteasome functions in mammals were still unclear. Therefore, I investigated the phenotypes of *KIAA0368*-deficient mice. *KIAA0368*-deficient mice were apparently normal and fertile in both male and female. Peptidase activities were not impaired *in vitro*. Proteasome structure were tested by sedimentation velocity centrifugation assay, but it seemed not to be altered. These data demonstrated that Ecm29 was not essential for development and viability of mice, and the proteasome function was not impaired by deficiency of *KIAA0368* in basal condition.

1.2 Introduction

Ecm29 is known to be the proteasome-associated protein. Ecm29 attaches on both the CP and the 19S RP (Leggett et al., 2002). CP-RP interaction was destabilized in the ATP deprived condition in *ecm29* deletion mutant (Kleijnen et al., 2007), therefore Ecm29 is thought to strengthen the tethering between 20S CP and 19S RP. On the other hand, other experiments suggested that Ecm29 has inhibitory effects against proteasome activity by inducing dissociation of CP-RP (Wang at al., 2010), or suppressing peptidase activities of aberrant proteasomes (Park et al., 2011, De La Mota-Peynado et al., 2013). It is also proposed that Ecm29 plays a role in a checkpoint during CP maturation (Lehmann et al., 2010). In mammals, Ecm29 is located on the cytosolic surface of secretory components such as endoplasmic reticulum and golgi body and plays a role in the regulation of proteasome localization and signaling pathway (Gorbea et al., 2004, Gorbea et al., 2010 and Gorbea et al., 2013).

Although Ecm29 in yeast has been reported to regulate the proteasomal CP-RP interactions, its physiological roles in mammals has not been analyzed. Therefore *KIAA0368*-deficient mice were generated and I investigated its phenotypes and effects on the activities of mammalian proteasome.

1.3 Materials and Methods

Generation of KIAA0368-deficient mice.

Mouse *KIAA0368* gene was obtained from C57BL/6J mouse genomic DNA library. The targeting vector was constructed by cloning the 13.5 kb *HindIII-HindIII* fragment, and the insertion of 1.2 kb neomycin resistant gene cassette. The diphtheria toxin A gene (DTA) was used for negative selection. TT2 ES cells were transfected with the targeting vector and selected by G418 (SIGMA). ES cells heterozygous for *KIAA0368* gene were microinjected to 8-cell stage ICR mice embryos to generate chimeric mice. Germline transmission of the mutant allele was identified by Southern blot analyses. Heterozygous mice were backcrossed for more than 10 generations on the C57BL/6J background. *KIAA0368* homozygous mice and their wild-type control littermates were obtained by heterozygous intercrossing. All animal care and experimental treatments were in accordance with the University of Tsukuba guidelines for animal care and use.

Genomic PCR

Tails from mice were lysed in DNA extraction buffer (50 mM Tris-HCl [pH 8.0], 100 mM NaCl, 20 mM ethylenediaminetetraacetic acid [EDTA], 1% SDS, 2 mg/ml proteinase E and 0.3 mg/ml proteinase K) at 55 ºC for overnight. DNA were purified by phenol / chloroform extraction followed by ethanol precipitation and resuspended in a buffer (10 mM Tris-HCl [pH8.0], 1 mM EDTA). Wild-type and mutant alleles were amplified by PCR using the primers listed in Table 1. Amplified DNA fragments were electrophoresed on 1% agarose gel at constant voltage of 200 V for 20 min. Gel was stained with ethidium bromide and visualized under UV-transilluminator.

Immunoblot analyses

Organs were homogenized using Potter-Elvehjem homogenizer in five times volume per organ weight of homogenization buffer (25 mM Tris-HCl [pH 7.5], 250 mM Sucrose, 1 mM dithiothreitol [DTT] and 1 mM phenylmethylsulfonyl fluoride [PMSF]) and centrifuged at 20,000 ×g for 30 min. Cells were lysed in ice-cold lysis buffer (50 mM Tris-HCl [pH 7.5], 5 mM $MgCl_2$, 2 mM ATP, 0.5% NP-40 and 1 mM DTT) and centrifuged at 15,000 ×g for 30 min. The supernatants were combined with SDS-PAGE sample buffer and boiled at 100 ºC for 5 min. Samples were subjected to SDS-PAGE and blotted onto PVDF membranes (PALL). Membranes were incubated in 5% non-fat dry milk in TBS-T (50 mM Tris-HCl [pH 7.5], 150 mM NaCl and 0.05% Tween 20) for blocking and treated with primary and secondary antibodies. Bands were visualized by Western Lightning Plus-ECL reagent (PerkinElmer Life Sciences).

Antibodies

Antibodies used in this study are listed in Table 2. Anti-Ecm29, anti-β7 and anti-PA200 antibodies were raised by immunizing His-tagged recombinant Ecm29 (N-terminal 100 amino acids), full length β7 and PA200 (N-terminal 100 amino acids) proteins in rabbit, respectively. The quality of the antibodies were checked by ELISA and immunoblot. Anti-PA28α and anti-Rpt1 antibodies are described previously (Tanahashi et al., 1997, Tanahashi et al., 1998). Peroxidase-conjugated anti-rabbit and anti-mouse IgG antibodies (Jackson ImmunoResearch) were used as secondary antibodies for immunoblot analyses. Anti-ubiquitin rabbit polyclonal (Dako; Z0458) and Alexa Fluor 488-conjugated anti-rabbit IgG (Invitrogen) antibodies were used for immunohistological analyses.

Sedimentation velocity centrifugation

1 mg of tissue lysates were separated by glycerol density gradient ultracentrifugation (25 mM Tris-HCl [pH 7.5], 10-40% Glycerol, 5 mM $MgCl_2$, 2 mM ATP and 1 mM DTT) at 25,000 r.p.m. with SW41Ti rotor for 22 h. The gradients were fractionated using liquid layer injector fractionator (ADVANTEC) equipped with fraction collector (ATTO) into 23 or 32 fractions.

Measurement of proteasome peptidase activity

10 μl of samples were incubated with 0.5 μM fluorogenic substrates in a final 100 μl of reaction mixture (50 mM Tris-HCl [pH 7.5], 25 mM KCl, 5 mM $MgCl_2$, 1 mM ATP with or without 0.02% SDS) at 37 ºC. Succinyl-Leu-Leu-Val-Tyr-7-amino-4-methylcoumarine (Suc-LLVY-AMC) (Peptide Institute) was used as fluorogenic substrates. The fluorescence were measured using Multi label counter (PerkinElmer Life Sciences) at 355 nm excitation and 460 nm emission wavelengths. The results show fluorescence per protein amounts and reaction time.

Histology

Wild-type and *KIAA0368*-deficient mice of 8 weeks old were fixed in 4% paraformaldehyde in phosphate buffered saline (PFA/PBS) by perfusion fixation. Fixed organs were paraffin embedded and sectioned at 2 μm. Sections were stained with haematoxylin and eosin (H&E) or subjected to immunohistochemical analyses.

Immunohistochemistry

Deparaffinized specimens were immersed in a citrate buffer (5 μM $C_6H_8O_7$ and 5 μM

$Na_3(C_6H_5O_7)$ [pH 6.0]) and boiled for 3 min to retrieve antigens. The activated tissues were blocked in 2% goat serum and incubated with anti-ubiquitin rabbit polyclonal antibody followed by Alexa Fluor 488-conjugated anti-rabbit antibody. The slides were mounted with VECTASHIELD® (Vector Laboratories) containing Hoechst 33342 (Life Sciences). The slides were observed using fluorescence microscope (Keyence, BZ-9000).

1.4 Results

KIAA0368-deficient mice were viable and grew normally.

To investigate the physiological roles of Ecm29, mice lacking *KIAA0368* gene were generated. The targeting vector was designed to replace exon 2 of the *KIAA0368* gene with neomycin resistant gene cassette (Fig. 1). The disruption of *KIAA0368* gene was confirmed by PCR of genomic DNA (Fig. 2). Heterozygous intercrossing yielded homozygous mice in predicted Mendelian ratio (Table 3). Tissue blot of Ecm29 revealed its protein expression in various organs and the homozygous mice lacked the expression of Ecm29 suggesting that the mutation is a null mutation. (Fig. 8, upper panel). The expression level of Ecm29 protein decreased dependent on the mutant gene dosage (Fig. 3). The *KIAA0368* homozygous mice grew normally, were fertile both male and female. Tissue morphologies on H&E staining were apparently normal at all major organs analyzed, such as cerebrum, heart, kidney, testis, liver, pancreas and spleen (Fig. 4).

Proteasomal activities were not impaired in KIAA0368-deficient mice.

I next measured proteasomal peptidase activities in tissue lysates of wild-type, heterozygous and homozygous mice for *KIAA0368* (Fig. 5). To measure the activities of latent 20S CP, 0.02% SDS was added to the reaction mixture as an artificial proteasome activator for latent 20S CP. Their peptidase activities were not significantly altered in *KIAA0368* homozygous mice compared to wild-type and heterozygous counterparts. To further confirm this, I separated the 26S proteasome by glycerol density gradient centrifugation. The peptidase activities of 26S proteasome in both wild-type and mutant

mice were observed at fractions 14-16, and their peptidase activities were comparable (Fig. 6). These results suggest that loss of *KIAA0368* does not affect peptidase activities of 26S proteasome.

Peptidase activities of proteasomes were not affected in lysates from *KIAA0368*-deficient mice, however, it may affect degradation of ubiquitylated proteins. Therefore I immunostained the tissue sections with ubiquitin antibody to check whether ubiquitin level is changed or ubiquitin-positive aggregates could be observed in *KIAA0368*-deficient mice. The staining pattern of ubiquitin was normal in *KIAA0368*-deficient mice as compared to wild-type mice (Fig. 7). The tissue blot of these organs also did not show marked differences in the amount of ubiquitylated protein (Fig. 8). These results suggest that proteasomal protein degradation is not impaired in *KIAA0368*-deficient tissues, although the possibility of some defects in proteasome function(s) in some organs cannot be ruled out.

Other Proteasome activators were not altered in KIAA0368-deficient mice.

Although the differences in peptidase activities and protein degradation were not observed between wild-type and *KIAA0368*-deficient mice, the expression of proteasome activators other than 19S RP and their interaction with CP might be affected by *KIAA0368* deletion. To this end, I analyzed the expression of proteasome activators in tissue lysates and glycerol density gradient-fractionated samples. The expression levels of PA28α, PA28γ and PA200 in tissue lysates were not altered in *KIAA0368*-deficient mice (Fig. 9). Next, those expressions on fractionated samples were analyzed (Fig. 10). In wild-type lysate, subunit of CP (β7 subunit) was sedimented in fraction 8-12. The peak of Ecm29 (fractions 10-14) was observed at overlapping but slightly

higher sedimentation fractions than those of β7 subunit. Subunit of 19S RP (Rpt1) was also distributed in higher sedimentation fractions (fractions 10-14). PA28αβ and γ complex were sedimented in the lower fractions (fractions 2-6), suggesting it was not associated to CP or dissociated during the centrifugation. PA200 was observed in fractions 8-12, similar to those of β7. In *KIAA0368*-deficient lysates, the subunit distributions were similar to those of wild-type counterpart, and any alteration was observed. These results demonstrate that 26S proteasome and the hybrid proteasome with PA200 is not impaired or affected by *KIAA0368*-deficiency.

1.5 Discussion

In this study, I reported the phenotypes of *KIAA0368*-deficient mice. *KIAA0368*-deficient mice were viable, fertile, and did not show any obvious histological abnormalities. Therefore Ecm29 is not essential for development and viability of mice.

Prior investigation reported that Ecm29 tethers both CP and 19S RP to stabilize the holoenzyme independent of ATP energy (Leggett et al., 2002). I did not observe the instability of CP-RP in *KIAA0368*-deficient mice (Fig. 10). The degradation of abnormal and ubiquitylated proteins was also not observed in *KIAA0368*-deficient mice (Fig. 7, 8).

Chapter 2

Regulation of proteasome under oxidative stress

2.1 Summary

Vast majority of intracellular and extracellular stresses are involved in various diseases. The ubiquitin-proteasome system is known to be important for cell protection against various stresses. Proteasomes respond to several stresses in order to remove damaged proteins efficiently. Thus, I investigated stress responses on *KIAA0368*-deficient cells and its effects on proteasomes. *KIAA0368*-deficient cells were more resistant to oxidative stress-induced cell death than wild-type counterparts. Oxidative stress induced the dissociation of 26S proteasome into 20S CP and 19S RP in wild-type cells. In contrast, dissociation of 26S proteasome was impaired in *KIAA0368*-deficient cells. This response correlated to efficient removal of oxidized proteins in *KIAA0368*-deficient cells. Thus, Ecm29 is involved in the dissociation process of 26S proteasome and the failure of the dissociation result in rapid elimination of damaged proteins.

2.2 Introduction

Cells were constantly exposed to various intracellular and extracellular stresses which often cause protein damages. Various stresses lead to modification on proteins, lipid and nucleic acids (Sedelnikova et al., 2010, Adibhatla et al., 2010, Bochkov et al., 2010). Oxidative stress causes carbonylation of protein, and the abnormal accumulation of such modified proteins is related to Alzheimer's disease, inflammatory bowel disease and age-related diseases such as proteopathy (Reznick and Packer, 1998, Smith et al., 1991, Liu-Brody et al., 1996, Page et al., 2010). Therefore cells have protective systems to eliminate damaged proteins. Ubiquitin-proteasome system plays pivotal roles in removal of aberrant proteins (Goldberg, 2003).

Several regulation of proteasomes against oxidative stress is known to protect cells from toxicity (Aiken et al., 2011). Prior work demonstrated that uncapped 20S CP is responsible for degradation of oxidatively damaged proteins because dissociation of 26S proteasome was induced by oxidative stress and ubiquitin-independent rapid degradation is facilitated in several stresses (Davies, 2001). On the other hand, other investigation reported 26S proteasome functions in removal of damaged proteins because ubiquitylation is upregulated by oxidative stress (Shang et al., 1997). PA28- and PA200-attached proteasomes and special proteasome called immunoproteasomes are also suggested to be important for efficient recognition and degradation of damaged proteins (Pickering and Davies, 2012, Seifert et al., 2010). However the exact mechanism on removal of oxidatively damaged proteins were remained unclear.

ecm29 deletion mutant was reported to be more sensitive to oxidative stress-induced cell death in yeast (Wang et al., 2010). However the weakness of oxidative stress-induced

cell death in *KIAA0368*-deficient cells and the regulation of proteasome to oxidative stress was not reported. Therefore, I investigated the response and regulation of proteasomes upon oxidative stress in *KIAA0368*-deficient cells.

2.3 Materials and Methods

Preparation of MEFs and cell culture

Mouse embryonic fibroblast (MEF) cells were isolated from 13.5 days post coitus embryos and cultured in Dulbecco's modified Eagle's medium (D-MEM, high glucose) (Wako) supplemented with 10% fetal bovine serum and 1% penicillin / streptomycin (Invitrogen) in 37 ºC, 5% CO_2 incubator. MEF cells were immortalized by transfecting SV40 large T antigen (kindly provided by N. Mizushima [Tokyo University]) using polyethyleneimine (Polyscience) according to the manufacturer's protocol.

Oxidative stress response

MEF cells were cultured in D-MEM containing various concentrations of H_2O_2 or H_2O as control for indicated periods in the presence or absence of 20 μM MG132 (Peptide Institute). Cells were subsequently subjected to cell viability assay and immunoblot analyses.

Cell viability assay

3×10^3 cells were cultured in 96-well plate and stimulated with various concentrations of H_2O_2 for 2 h. After stimulation, medium was replaced with fresh complete medium and incubated for 16 h. Viable cells were measured by Cell Counting Kit-8 (Dojindo). The absorbance was measured at 450 nm. For trypan-blue exclusion assay, 1×10^5 cells were incubated in various concentrations of H_2O_2 for 2 h. After incubation, cells were trypsinized and mixed with equal volumes of 0.4% trypan-blue solution (SIGMA). Cells were counted on burkerturk hemocytometer, and the ratio of the blue-stained dead cells

per total cells were calculated.

DNA ladder assay

1×10^6 cells were incubated with various concentrations of H_2O_2 for 24 h. Cells were harvested and lysed in DNA extraction buffer (50 mM Tris-HCl [pH 8.0], 100 mM NaCl, 20 mM EDTA, 1% SDS, 2 mg/ml proteinase E and 0.3 mg/ml proteinase K) at 55 ºC for overnight. DNA were purified by phenol / chloroform extraction followed by ethanol precipitation and resuspended in a buffer (10 mM Tris-HCl [pH8.0], 1 mM EDTA and 0.2 mg/ml RNase A). 0.5 μg of DNA were electrophoresed on 1% agarose gel at constant voltage of 200 V for 10 min. Gel was stained with ethidium bromide and visualized under UV-transilluminator.

Measurement of carbonylated protein

Carbonyl groups were detected as a marker of damaged proteins (Dalle-Donne et al., 2003). Cells were lysed in RIPA buffer (50 mM Tris-HCl [pH 7.5], 150 mM NaCl, 1% NP-40, 1% Sodium deoxycholate, 0.1% SDS and 2 mM DTT). 5 μl of lysates were denatured by adding 5 μl of 12% SDS and incubated for 5 min at room temperature. Samples were incubated with 5 μl of 2.5 mM 2,4-dinitrophenylhydrazine dissolved in 2.5% trifluoroacetic acid for 15 min for derivatization, and the reaction was stopped by adding 7.5 μl of 500 μM Tris and 10% glycerol. 7.5 μg of samples were subjected to immunoblot analyses using anti-DNP antibody.

Immunocytochemistry

Cells were cultured on coverslips and were exposed to 200 μM H_2O_2 and/or 20 μM

MG132. The cells were fixed in 4% PFA in PBS for 30 min, permeabilized in 0.1% Triton X-100 in PBS for 30min, and derivatized in 0.1 mg/ml DNPH in 2 N HCl for 30 min. The coverslips were then immersed in primary antibodies diluted in 1% BSA, 0.1% Tween 20 in PBS followed by secondary immunofluorescent antibodies diluted in 1% BSA, 0.1% Tween 20 in PBS. Nuclei were stained with Hoechst 33342 (Life Sciences). The coverslips were mounted onto slides using Fluoromount/Plus mounting solution (Diagnostic BioSystems) and images were obtained using a fluorescent microscope (Keyence, BZ-9000).

2.4 Results

KIAA0368-deficient cells were resistant to oxidative stress.

Prior investigation in yeast reported that yeast lacking *ecm29* is sensitive to oxidative stress (Wang et al., 2010). Therefore, I analyzed the cell viability and apoptosis using MEF cells derived from *KIAA0368*-deficient mice and wild-type littermate control, following H_2O_2 treatment. At all points of H_2O_2 concentrations, *KIAA0368*-deficient cells were more resistant to H_2O_2 than wild-type counterparts (Fig. 11). The H_2O_2-induced cell death was also analyzed by trypan blue exclusion assay (Fig. 12). About 20% of cells were dead by 50 μM H_2O_2 treatment in wild-type cells. However, only 4% of cells were dead even by 200 μM H_2O_2 treatment in *KIAA0368*-deficient cells. These results indicate *KIAA0368*-deficient cells are more resistant to H_2O_2-induced cell death than wild-type counterparts. When the DNA fragmentation was also analyzed, apoptosis-induced DNA fragmentation was detected at 200 μM H_2O_2 on wild-type cells, but only at higher concentration in *KIAA0368*-deficient cells (Fig. 13). Taken together, *KIAA0368*-deficient cells were more tolerant to oxidative stress-induced cell death.

Disassembly of proteasomes under oxidative stress was impaired in KIAA0368-deficient cells.

To test whether the oxidative stress tolerance is associated with any change in the proteasome composition, the sedimentation of CP and 19S RP under oxidative stress were analyzed. Wild-type and *KIAA0368*-deficient MEF cells treated with H_2O_2 were subjected to glycerol density gradient fractionation followed by immunoblot analyses (Fig. 14). At untreated normal condition, subunit of CP (β5) was sedimented around 16-

22 fractions, and subunit of 19S RP (Rpt1) appeared at lower fraction and higher fractions (fractions 8-12 and 20-22) in both wild-type and *KIAA0368*-deficient cells. Rpt1 in fractions 8-12 appears to be 19S RP complex, and fractions 20-22 to be 26S proteasome. Note that the 19S RP complex in lighter fractions was not detected in tissue lysate (Figs. 10, and 14). It is known that tissues contain more 26S proteasome than proliferating cells, and the appearance of free lid complex may be associated with the cell proliferation (Tai et al., 2010). Ecm29 was detected at wider range of fractions (fractions 7-29). After exposure to H_2O_2, Rpt1 was almost completely lost from the 26S fractions (fractions 20-22) on wild-type cells. These results suggest the possibility that 26S proteasome dissociates into 19S RP complex and CP in wild-type cells. On the other hand, Rpt1 still located at 26S fractions in *KIAA0368*-deficient cells after treatment of oxidants (fractions 20-22, Fig. 14 bottom 2 panels). These results suggest that the disassembly of 26S proteasome by the exposure of H_2O_2 is affected by the absence of Ecm29. The decrease in proteasomal peptidase activity on 26S fractions was also observed in wild-type, but not mutant MEF cells (Fig. 15, fraction 20), supporting the notion that 26S proteasome is dissociated and inactivated in wild-type cells but not *KIAA0368*-deficient cells.

Degradation of carbonylated proteins were accelerated in KIAA0368-deficient cells.

Oxidative stress is apprehended as to induce the formation of toxic misfolded proteins (Stadtman, 2006). To assess the effect of proteasome dissociation on degradation of damaged protein, we analyzed the amount of carbonylated proteins (Dalle-Donne et al., 2003). After exposure to H_2O_2, carbonylated proteins were immediately accumulated on wild-type cells, and subsequently decreased by 360 min post stimulation (Fig. 16, upper

panel). The ubiquitin blots also show the accumulation of ubiquitylated proteins and their subsequent degradation in wild-type cells. These results indicate that protein carbonylation and ubiquitylation are upregulated by exposure to oxidative stress, and they are slowly subjected to degradation in wild-type cells. On the other hand, the accumulation of carbonylated proteins nor ubiquitylated proteins were not observed in *KIAA0368*-deficient cells (Fig. 16). These results suggest that carbonylated proteins are efficiently degraded by 26S proteasome in *KIAA0368*$^{-/-}$ cells. To test whether proteasomes were reconstructed after 360 min of stimulation, proteasome compositions were analyzed by sedimentation velocity fractionation. The dissociation of 26S proteasome in wild-type cells were restored in 360 min H_2O_2 exposure (Fig. 17). Taken together, *KIAA0368*-deficiency leads to efficient degradation of damaged and ubiquitylated proteins due to stabilized 26S proteasome under oxidative stress.

I next assessed whether the rapid degradation of carbonylated and ubiquitylated proteins in *KIAA0368*-deficiency were dependent on proteasome, accumulation of carbonylated and ubiquitylated proteins were stained in the presence of proteasome inhibitor MG132 (Fig. 18). By H_2O_2 exposure, accumulation of carbonylated and ubiquitylated proteins were fewer in *KIAA0368*$^{-/-}$ cells compared to wild-type cells. When MG132 was added during H_2O_2 treatment, both carbonylated and ubiquitylated proteins were accumulated in *KIAA0368*-deficient cells. To confirm that this efficient degradation is indeed dependent on proteasome, levels of ubiquitylated proteins were detected in the presence of MG132. In the presence of MG132, H_2O_2-induced accumulation of ubiquitylated proteins were observed even in *KIAA0368*$^{-/-}$ cells (Fig. 19). Therefore, the proteasome has significant contribution to efficient degradation of damaged proteins. Taken together, *KIAA0368*-deficiency leads to efficient degradation of damaged and

ubiquitylated proteins due to stabilized 26S proteasome under oxidative stress.

2.5 Discussion

In this chapter, I unexpectedly observed the stabilization of 26S proteasome under oxidative stress condition. In yeast, Ecm29 recognizes immature proteasome species and functions as a scaffold for CP maturation (Lehmann et al., 2010). According to the model that Ecm29 is involved in the proteasome maturation checkpoint, it is possible that other protein(s) associated with the 26S proteasome confer the stability of the 26S proteasome in the absence of Ecm29.

Previous investigation demonstrated that yeast lacking *ecm29* was more sensitive to oxidative stress (Wang et al., 2010). On the contrary, our experiment demonstrated that *KIAA0368*-deficient cells were more resistant to oxidative stress (Figs. 12 and 13). In yeast, Ecm29 was reported to function in *de novo* synthesis of CP (Lehmann et al., 2010), while we could not observe defects in proteasome assembly and maturation (Fig. 6). Therefore, the difference in cell viability may be associated to the different requirement of Ecm29 on *de novo* synthesis of CP, which is responsible for efficient degradation of damaged proteins.

Several investigations reported that, 20S CP (Davies, 2001), immunoproteasome (Seifert et al., 2010), 26S proteasome (Shang et al., 1997), PA28- and PA200-conjugated proteasomes (Pickering and Davies, 2012) are responsible for efficient recognition and degradation of oxidatively damaged proteins. In support of the importance of proteasomes other than 26S proteasome, my data demonstrated dissociation of 26S proteasome in wild-type cells (Fig. 14). However my data presented that the elimination of damaged proteins was faster in *KIAA0368*-deficient cells (Fig. 16). These results suggest that, even though 20S CP can degrade oxidatively damaged proteins, and the contribution of other

PA28-, and PA200- conjugated proteasomes cannot be ruled out, 26S proteasome is more competent to efficiently eliminate damaged proteins.

General Discussion

According to the analyses using *KIAA0368*-deficient mice, obvious phenotypes were not observed in my experiment. However, *KIAA0368*-deficient cells showed impaired proteasome regulation upon H_2O_2 treatment (Fig. 14). Therefore, *KIAA0368*-deficient mice might show abnormalities by oxidative stress. This investigation is under way.

My experiments provided the possibility that Ecm29 functions on the dissociation of 26S proteasome. The consequence and the factors related to 26S proteasome dissociation was not identified up to date, therefore further investigation is required to elucidate the effect of the defects of 26S proteasome dissociation. The Ecm29 study will provide clues to analyze the detailed mechanism of 26S proteasome dissociation.

I unveiled efficient degradation of carbonylated and ubiquitylated proteins in *KIAA0368*-deficient cells (Fig. 16). Because oxidative stress is involved in numerous diseases (Reznick and Packer, 1998, Smith et al., 1991, Liu-Brody et al., 1996, Aiken et al., 2011, Page et al., 2010), Ecm29 has the possibility for the potential target for therapy. In this context, my data provide the notion that Ecm29 is not important for cell protection against stresses. Previous investigation reported that Ecm29 negatively regulates aberrant proteasomes which have too high peptidase activities in yeast (Park et al., 2011). According to this report, Ecm29 might inhibit aberrant proteasomes induced by oxidative stress. Take account of this, the accumulation of aberrant proteasomes and the consequence of aberrant proteasomes should be examined using *KIAA0368*-deficient cells.

A large part of Ecm29 protein is composed of HEAT-like repeat motifs. Like Ecm29, proteasome activator PA200 is also composed of HEAT-like motifs (Kajava et al., 2004).

It was previously reported that both Ecm29 and Blm10 (yeast homologue of PA200) function in CP assembly pathways (Lehmann et al., 2010, Fehlker et al., 2003) and that deletion of both *ecm29* and *blm10* shows synthetic sensitivities to high temperature and canavanine-induced proteotoxicity in yeast (Schmidt et al., 2005). In this regard, although we did not observe the up-regulation of PA200 in the mutant mice, *KIAA0368*-deficiency might be compensated in part by PA200. The analysis of double knockout mice lacking both *KIAA0368* and *Psme4* would be important, which is under investigation.

Acknowledgements

First of all, I would like to thank Prof. T. Chiba for his excellent supervision, assignment of the workplace and for his encouragement throughout the program.

I would like to thank Assist. Prof. F. Tsuruta and Assist. Prof. T. Naganuma for their help as second supervisors.

I also thank all members of the Chiba laboratory for technical support, hospitality, and the helpful discussions.

References

Adibhatla, R.M., Hatcher J.F. (2010) Lipid oxidation and peroxidation in CNS health and disease: from molecular mechanisms to therapeutic opportunities. *Antioxid. Redox. Signal.* 12, 125–169

Aiken C.T., Kaake R.M., Wang X., Huang L. (2011) Oxidative Stress-Mediated Regulation of Proteasome Complexes. *Mol. Cell. Proteomics* 10, R110.006924

Bochkov V.N., Oskolkova O.V., Birukov K.G., Levonen A.L., Binder C.J., Stöckl J. (2010) Generation and biological activities of oxidized phospholipids. *Antioxid. Redox. Signal.* 12, 1009–1059

Dalle-Donne I., Rossi R., Giustarini, D., Milzani A., Colombo R. (2003) Protein carbonyl groups as biomarkers of oxidative stress. *Clin. Chim. Acta.* 40, 23-38

Davies K.J. (2001) Degradation of oxidized proteins by the 20S proteasome. *Biochimie* 83, 301-310

De La Mota-Peynado A., Lee S.Y., Pierce B.M., Wani P., Singh C.R., Roelofs J. (2013) The proteasome-associated protein Ecm29 inhibits proteasomal ATPase activity and in vivo protein degradation by the proteasome. *J. Biol. Chem.* 288, 29467-29481

Deveraux Q., Ustrell V., Pickart C., Rechsteiner M. (1994) A 26 S protease subunit that

binds ubiquitin conjugates. *J. Biol. Chem.* 269, 7059-7061

Dick T.P., Ruppert T., Groettrup M., Kloetzel P.M., Kuehn L., Koszinowski U.H., Stevanović S., Schild H., Rammensee H.G. (1996) Coordinated dual cleavages induced by the proteasome regulator PA28 lead to dominant MHC ligands. *Cell* 86, 253-262

Fehlker M., Wendler P., Lehmann A., Enenkel C. (2003) Blm3 is part of nascent proteasomes and is involved in a late stage of nuclear proteasome assembly. *EMBO Rep.* 4, 959-963

Finley D. (2002) Ubiquitin chained and crosslinked. *Nat. Cell. Biol.* 4, E121-E123

Gavin A.C., Bösche M., Krause R., Grandi P., Marzioch M., Bauer A., Schultz J., Rick J.M., Michon A.M., Cruciat C.M., Remor M., Höfert C., Schelder M., Brajenovic M., Ruffner H., Merino A., Klein K., Hudak M., Dickson D., Rudi T., Gnau V., Bauch A., Bastuck S., Huhse B., Leutwein C., Heurtier M.A., Copley R.R., Edelmann A., Querfurth E., Rybin V., Drewes G., Raida M., Bouwmeester T., Bork P., Seraphin B., Kuster B., Neubauer G., Superti-Furga G. (2002) Functional organization of the yeast proteome by systematic analysis of protein complexes. *Nature* 415, 141-147

Goldberg A.L. (1990) ATP-dependent proteases in prokaryotic and eukaryotic cells. *Semin. Cell Biol.* 1, 423-432

Goldberg A.L. (2003) Protein degradation and protection against misfolded or damaged

proteins. *Nature* 426, 895-899

Gorbea C., Goellner G.M., Teter K., Holmes R.K., Rechsteiner M. (2004) Characterization of mammalian Ecm29, a 26 S proteasome-associated protein that localizes to the nucleus and membrane vesicles. *J. Biol. Chem.* 279, 54849-54861

Gorbea C., Pratt G., Ustrell V., Bell R., Sahasrabudhe S., Hughes R.E., Rechsteiner M. (2010) A protein interaction network for Ecm29 links the 26 S proteasome to molecular motors and endosomal components. *J. Biol. Chem.* 285, 31616-31633

Gorbea C., Rechsteiner M., Vallejo J.G., Bowles N.E. (2013) Depletion of the 26S proteasome adaptor Ecm29 increases Toll-like receptor 3 signaling. *Sci. Signal.* 6, ra86

Groettrup M., Soza A., Eggers M., Kuehn L., Dick T.P., Schild H., Rammensee H.G., Koszinowski U.H., Kloetzel P.M. (1996) A role for the proteasome regulator PA28alpha in antigen presentation. *Nature* 381, 166-168

Groll M., Ditzel L., Löwe J., Stock D., Bochtler M., Bartunik H.D., Huber R. (1997) Structure of 20S proteasome from yeast at 2.4 Å resolution. *Nature* 386, 463-471

Groll M., Bajorek M., Köhler A., Moroder L., Rubin D.M., Huber R., Glickman M.H., Finley D. (2000) A gated channel into the proteasome core particle. *Nat. Struct. Biol.* 7, 1062-1067

Heinemeyer W., Ramos P.C., Dohmen R.J. (2004) The ultimate nanoscale mincer: assembly, structure and active sites of the 20S proteasome core. *Cell. Mol. Life Sci.* 61, 1562–1578

Hershko A., Ciechanover A. (1998) The ubiquitin system. *Annu. Rev. Biochem.* 67, 425-479

Kajava A.V., Gorbea C., Ortega J., Rechsteiner M., Steven A.C. (2004) New HEAT-like repeat motifs in proteins regulating proteasome structure and function. *J. Struct. Biol.* 146, 425-430

Kleijnen M.F., Roelofs J., Park S., Hathaway N.A., Glickman M., King R.W., Finley D. (2007) Stability of the proteasome can be regulated allosterically through engagement of its proteolytic active sites. *Nat. Struct. Mol. Biol.* 14, 1180-1188

Köhler A., Cascio P., Leggett D.S., Woo K.M., Goldberg A.L., Finley D. (2001) The axial channel of the proteasome core particle is gated by the Rpt2 ATPase and controls both substrate entry and product release. *Mol. Cell* 7, 1143-1152

Lam Y.A., Lawson T.G., Velayutham M., Zweler J.L., Pickart C.M. (2002) A proteasomal ATPase subunit recognizes the polyubiquitin degradation signal. *Nature* 416, 763-767

Leggett D.S., Hanna J., Borodovsky A., Crosas B., Schmidt M., Baker R.T., Walz T., Ploegh H., Finley D. (2002) Multiple associated proteins regulate proteasome structure

and function. *Mol. Cell* 10, 495-507

Lehmann A., Niewienda A., Jechow K., Janek K., Enenkel C. (2010) Ecm29 fulfils quality control functions in proteasome assembly. *Mol. Cell* 38, 879-888

Lih-Brody L., Powell S.R., Collier K.P., Reddy G.M., Cerchia R., Kahn E., Weissman G.S., Katz S., Floyd R.A., McKinley M.J., Fisher S.E., Mullin G.E. (1996) Increased oxidative stress and decreased antioxidant defenses in mucosa of inflammatory bowel disease. *Dig. Dis. Sci.* 41, 2078-2086

Lussier M., White A.M., Sheraton J., di Paolo T., Treadwell J., Southard S.B., Horenstein C.I., Chen-Weiner J., Ram A.F., Kapteyn J.C., Roemer T.W., Vo D.H., Bondoc D.C., Hall J., Zhong W.W., Sdicu A.M., Davies J., Klis F.M., Robbins P.W., Bussey H. (1997) Large scale identification of genes involved in cell surface biosynthesis and architecture in Saccharomyces cerevisiae. *Genetics.* 147, 435-450

Mizushima N., Komatsu M. (2011) Autophagy: renovation of cells and tissues. *Cell* 147, 728-741

Murata S., Kawahara H., Tohma S., Yamamoto K., Kasahara M., Nabeshima Y., Tanaka K., Chiba T. (1999) Growth retardation in mice lacking the proteasome activator PA28gamma. *J. Biol. Chem.* 274, 38211-38215

Page M.M., Robb E.L., Salway K.D., Stuart J.A. (2010) Mitochondrial redox metabolism:

aging, longevity and dietary effects. *Mech. Ageing Dev.* 131, 242-252

Park S., Kim W., Tian G., Gygi S.P., Finley D. (2011) Structural defects in the regulatory particle-core particle interface of the proteasome induce a novel proteasome stress response. *J. Biol. Chem.* 286, 36652-36666

Pickering A.M., Davies K.J. (2012) Differential roles of proteasome and immunoproteasome regulators Pa28αβ, Pa28γ and Pa200 in the degradation of oxidized proteins. *Arch. Biochem. Biophys.* 523, 181-190

Qian M.X., Pang Y., Liu C.H., Haratake K., Du B.Y., Ji D.Y., Wang G.F., Zhu Q.Q., Song W., Yu Y., Zhang X.X., Huang H.T., Miao S., Chen L.B., Zhang Z.H., Liang Y.N., Liu S., Cha H., Yang D., Zhai Y., Komatsu T., Tsuruta F., Li H., Cao C., Li W., Li G.H., Cheng Y., Chiba T., Wang L., Goldberg A.L., Shen Y., Qiu X.B. (2013) Acetylation-mediated proteasomal degradation of core histones during DNA repair and spermatogenesis. *Cell* 153, 1012-1024

Reznick A.Z., Packer L. (1998) Oxidative damage to proteins: spectrophotometric method for carbonyl assay. *Methods Enzymol.* 233, 357-363

Schmidt M., Haas W., Crosas B., Santamaria P.G., Gygi S.P., Walz T., Finley D. (2005) The HEAT repeat protein Blm10 regulates the yeast proteasome by capping the core particle. *Nat. Struct. Mol. Biol.* 12, 294-303

Sedelnikova O.A., Redon C.E., Dickey J.S., Nakamura A.J., Georgakilas A.G., Bonner W.M. (2010) Role of oxidatively induced DNA lesions in human pathogenesis. *Mutant Res.* 704, 152-159

Seifert U., Bialy L.P., Ebstein F., Bech-Otschir D., Voigt A., Schröter F., Prozorovski T., Lange N., Steffen J., Rieger M., Kuckelkorn U., Aktas O., Kloetzel P.M., Krüger E. (2010) Immunoproteasomes preserve protein homeostasis upon interferon-induced oxidative stress. *Cell* 142, 613-624

Shang F., Gong X., Taylor A. (1997) Activity of ubiquitin-dependent pathway in response to oxidative stress: ubiquitin-activating enzyme is transiently up-regulated. *J. Biol. Chem.* 272, 23086-23093

Smith C.D., Carney J.M., Starke-Reed P.E., Oliver C.N., Stadtman E.R., Floyd R.A., Markesbery W.R. (1991) Excess brain protein oxidation and enzyme dysfunction in normal aging and in Alzheimer disease. *Proc. Natl. Acad. Sci. USA* 88, 10540-10543

Stadtman E.R. (2006) Protein oxidation and aging. *Free Radic. Res.* 40, 1250-1258

Stadtmueller B.M., Hill C.P. (2011) Proteasome activators. *Mol. Cell* 41, 8-19

Tai HC, Besche H, Goldberg AL, Schuman EM. (2010) Characterization of the brain 26S proteasome and its interacting proteins. *Front. Mol. Neurosci.* 3, 12

Tanahashi N., Yokota K., Ahn J.Y., Chung C.H., Fujiwara T., Takahashi E., DeMartino G.N., Slaughter C.A., Toyonaga T., Yamamura K., Shimbara N., Tanaka K. (1997) Molecular properties of the proteasome activator PA28 family proteins and gamma-interferon regulation. *Genes Cells* 2, 195-211

Tanahashi N., Suzuki M., Fujiwara T., Takahashi E., Shimbara N., Chung C.H., Tanaka K. (1998) Chromosomal localization and immunological analysis of a family of human 26S proteasomal ATPases. *Biochem. Biophys. Res. Commun.* 243, 229-232

Walczak-Jedrzejowska R., Wolski J.K., Slowikowska-Hilczer J. (2013) The role of oxidative stress and antioxidants in male fertility. *Cent European J Urol.* 66, 60-67

Wang X., Yen J., Kaiser P., Huang L. (2010) Regulation of the 26S proteasome complex during oxidative stress. *Sci. Signal.* 3, ra88

Whitby F.G., Masters E.I., Kramer L., Knowlton J.R., Yao Y., Wang C.C., Hill C.P. (2000) Structural basis for the activation of 20S proteasomes by 11S regulators. *Nature* 408, 115-120

Tables and Figures

Table 1 | Primers used in this study.

Product	Primer Name	Sequence
KIAA0368	11791 fwd	CCAGTGTAGC AGGAGTTCTT TCAGG
	14043 rev	CATATTTGGT TTTAGATCAG TCCAG
	Neo 460-483	GATCAGGATG ATCTGGACGA AGAG

Table 2 | Antibodies used in this study.

Name	Clone	Manufactuer
anti-Ecm29	-	This study
anti-β5	ab3330	Abcam
anti-β7	-	This study
anti-Rpt1	-	Tanahashi et al., 1998
anti-PA28α	-	Tanahashi et al., 1997
anti-PA28γ	611180	BD Transduction Laboratories
anti-PA200	-	This study
anti-ubiquitin	Z0458	Dako
anti-multi ubiquitin	FK2	MBL
anti-DNP	A150-117A	Bethyl Laboratories
anti-α-Tubulin	T9026	Sigma

Sex		Genotype +/+	+/-	-/-	Total
Male	numbers	77	116	74	267
	ratio (%)	28.8	43.4	27.7	50.7
Female	numbers	67	133	60	260
	ratio (%)	25.8	51.2	23.1	49.3
Total	numbers	144	249	134	527
	ratio (%)	27.3	47.2	25.4	100.0

Table 3 | Number of offspring yielded from heterozygous intercrossing.

The numbers and ratio of offspring corresponding to their sex and genotype produced from heterozygous intercrossing. Data were acquired from 63 mating pairs.

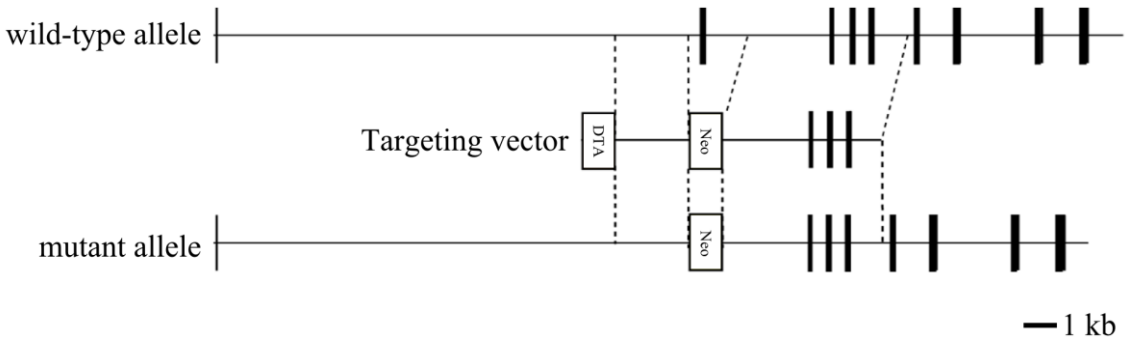

Figure 1 | Construct of *KIAA0368*-deficient mice.

Schematic structure of *KIAA0368* wild-type allele, the targeting vector, and the resulting mutant allele. The exons are illustrated by black boxes. Neo; neomycin-resistant gene cassette, DTA; diphtheria toxin A. Bar indicates 1 kb.

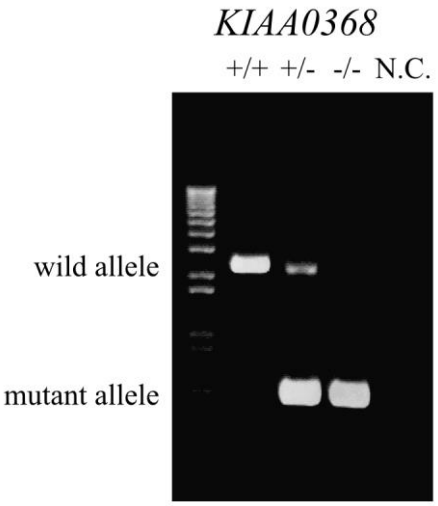

Figure 2 | Determination of mice genotypes by genomic PCR.

Detection of wild-type and mutant allele by genomic PCR. Tail genomic DNAs were subjected to PCR. Wild-type allele was detected at 2.2 kb and the mutant allele at 0.6 kb. NC; negative control.

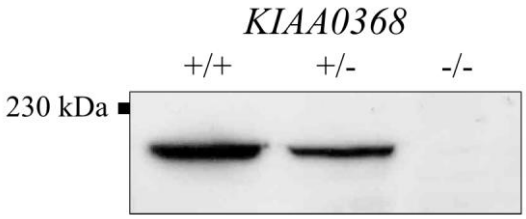

Figure 3 | Immunoblot of Ecm29 in wild-type, heterozygous and homozyogous to *KIAA0368*.

Detection of Ecm29 protein by immunoblotting. 50 μg of brain lysates of indicated genotypes were subjected to immunoblotting using antibody against Ecm29.

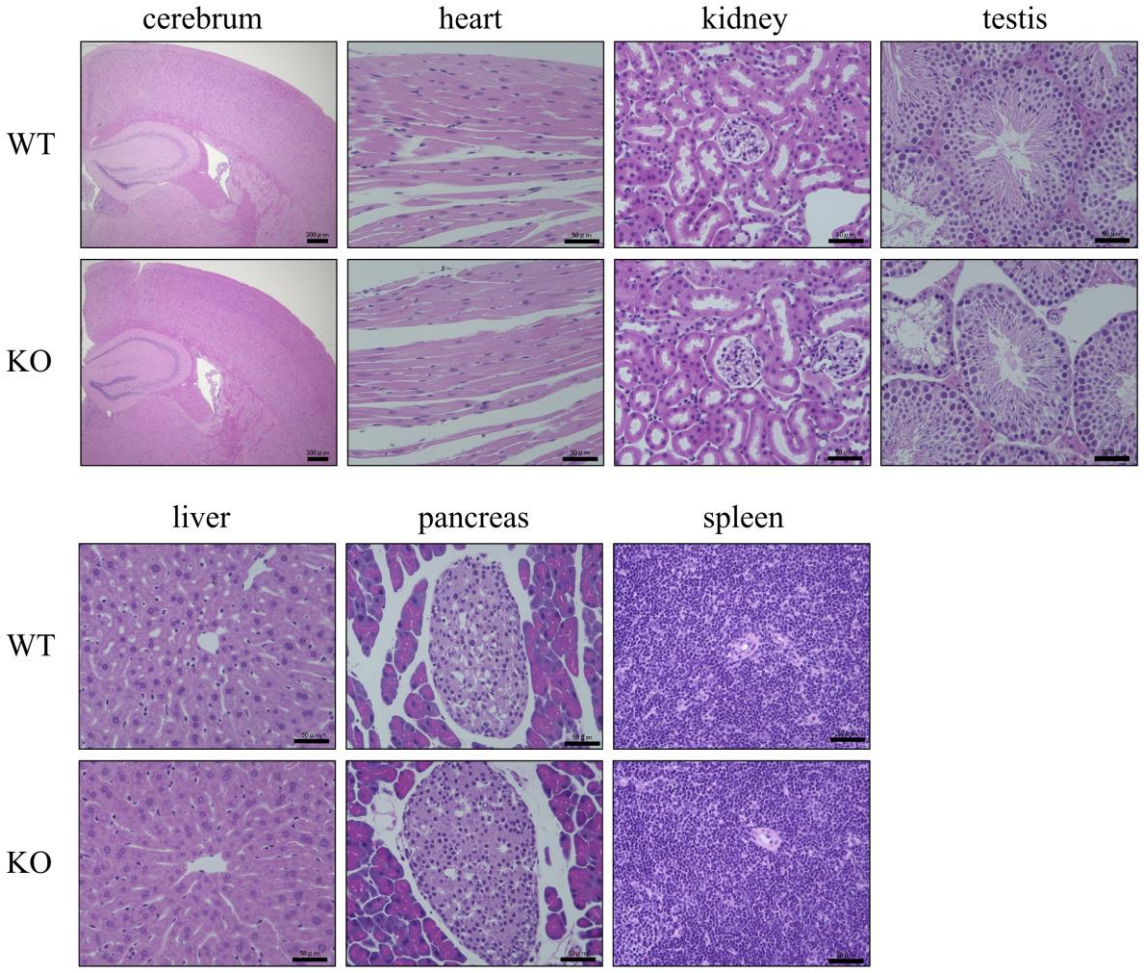

Figure 4 | Histology of *KIAA0368*-deficient mice.

Cerebrum, heart, kidney, testis, liver, pancreas and spleen sections from 8-weeks old wild-type (WT) and *KIAA0368*-deficient mice (KO). The tissue sections were stained with H&E. Scale bars in cerebrum indicates 300 μm, and others indicate 50 μm.

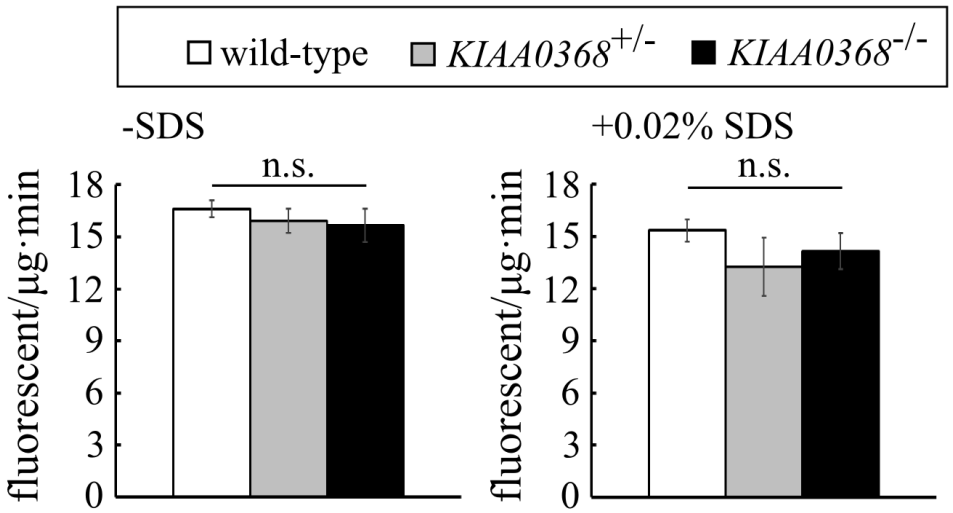

Figure 5 | Peptidase activities of *KIAA0368*-deficient mice.

Peptidase activities of testes lysates. 100 μg of testes lysates from wild-type, heterozygous or homozygous mice for *KIAA0368*, were incubated with fluorescent substrates in the presence or absence of 0.02% SDS. The bar charts represent the mean ± S.D. of fluorescence/μg/min. LLVY; chymotrypsin-like activity. White bars; wild-type, gray bars; *KIAA0368*$^{+/-}$, black bars; *KIAA0368*$^{-/-}$. n.s.; not significant by student's *t*-test.

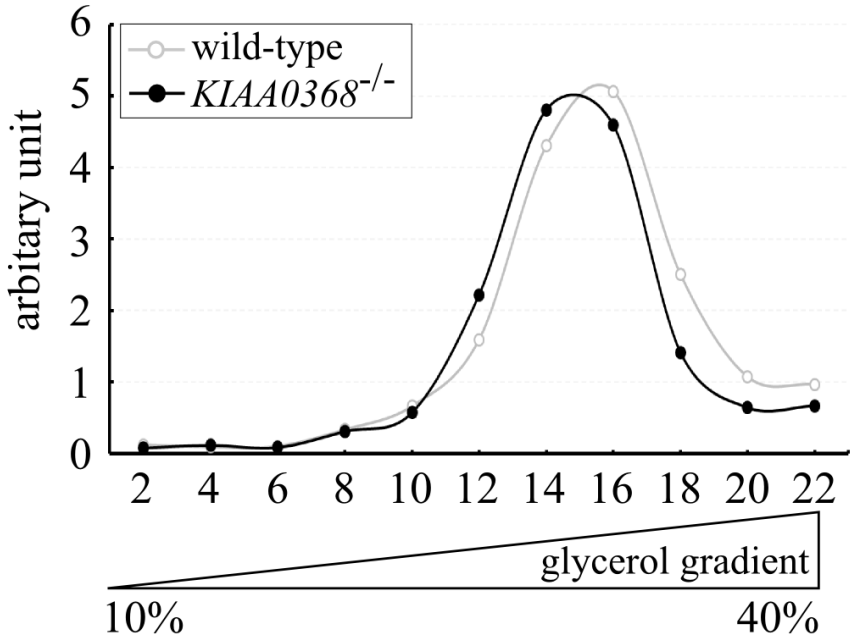

Figure 6 | Peptidase activities on sedimentation gradients.

Peptide hydrolysis activities of sedimentation velocity fractions from wild-type or *KIAA0368*-deficient testes lysates. 1 mg of testis lysates were fractionated by glycerol density gradient centrifugation (10-40% glycerol from 1 to 22 fractions). Suc-LLVY-AMC was used to measure the peptidase activities. The relative peptidase activities (fluorescence/min) normalized to the first fraction are shown.

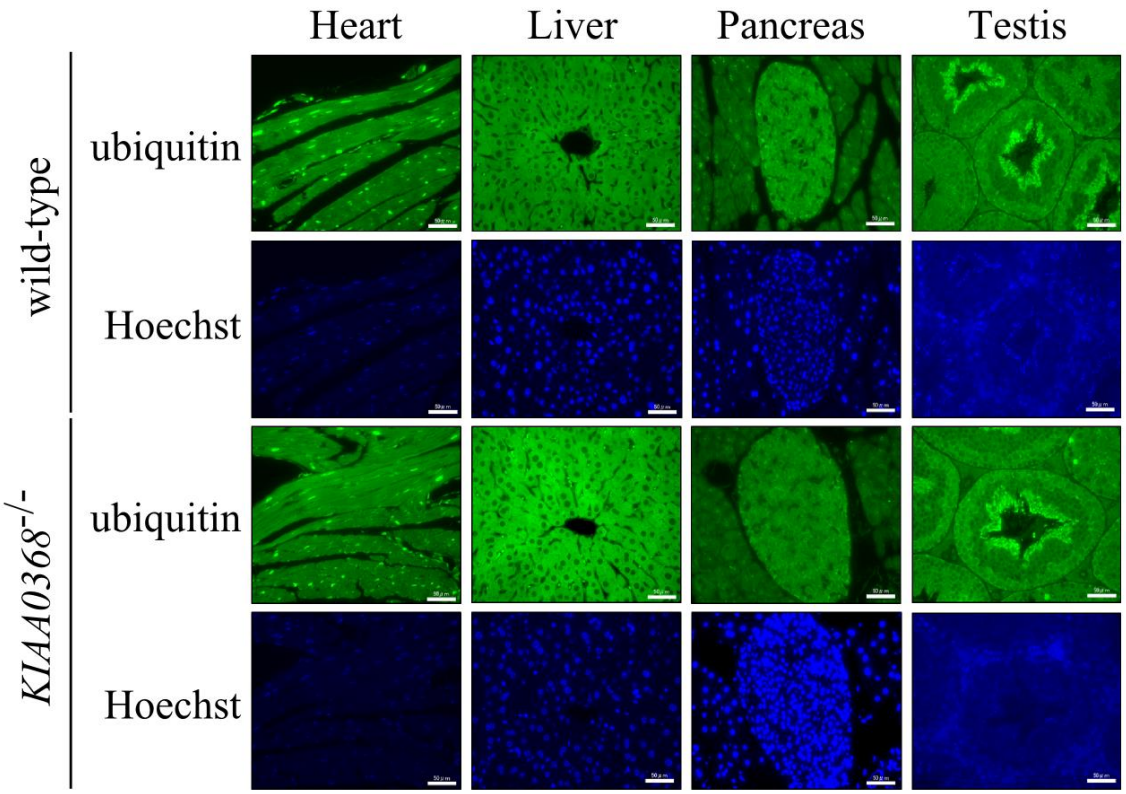

Figure 7 | Ubiquitin staining on *KIAA0368*-deficient mice tissues,

Tissue sections from wild-type or *KIAA0368*-deficient mice were immunostained with ubiquitin antibody and counterstained with Hoechst 33342. Scale bars indicate 50 μm.

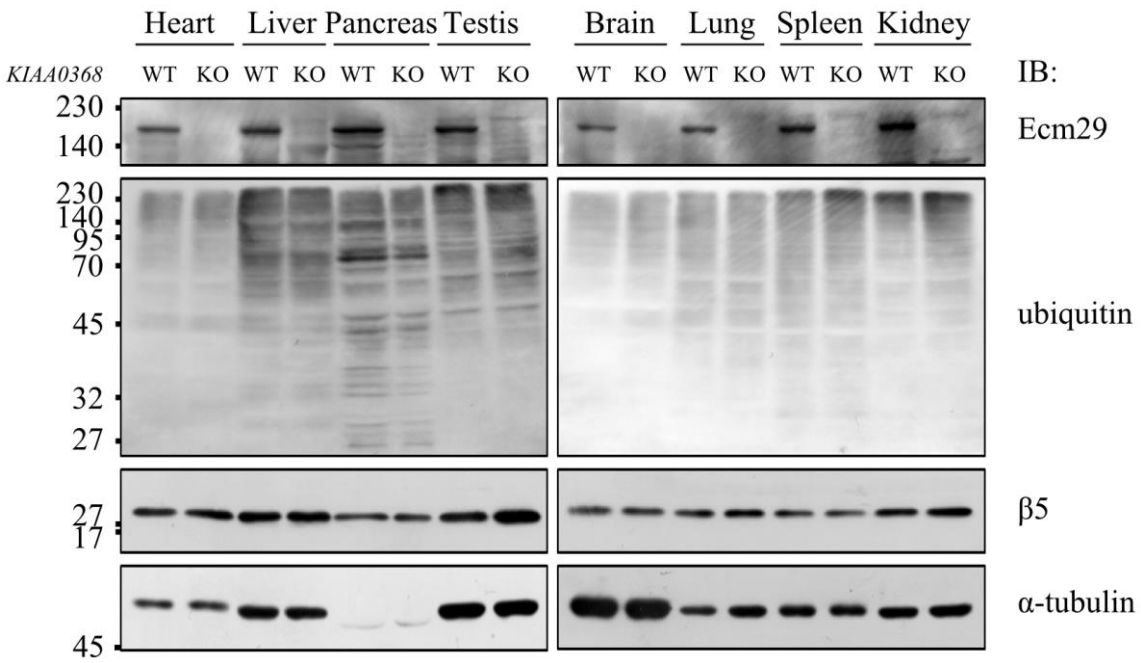

Figure 8 | Tissue blots of *KIAA0368*-deficient mice.

Tissue blots of wild-type (WT) and *KIAA0368*-deficient mice (KO). 50 μg of heart, liver, pancreas, testis, brain, lung, spleen and kidney lysates were subjected to immunoblot analyses using antibodies against Ecm29, Multi-ubiquitin, β5 and α-tubulin.

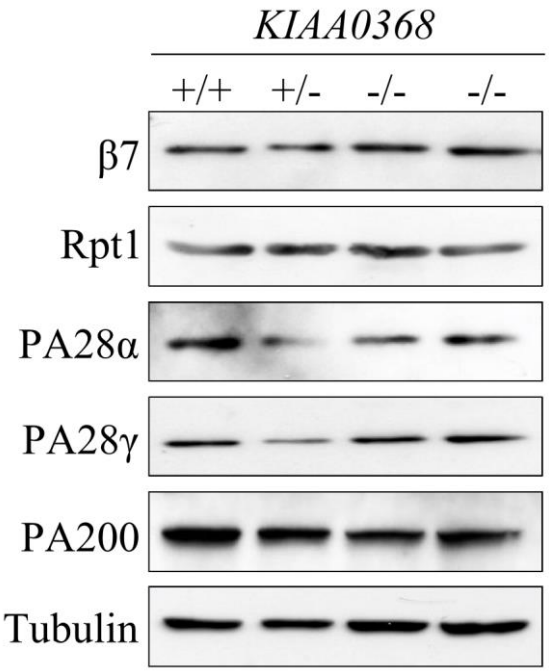

Figure 9 | Expression levels of proteasome components.

Expressions of CP subunit (β7) and proteasome activators (Rpt1, PA28α, PA28γ and PA200) in each *KIAA0368* wild-type (+/+), heterozygous (+/-) and homozygous (-/-) littermates. 20 μg of testis lysates of each genotype were subjected to immunoblot analyses.

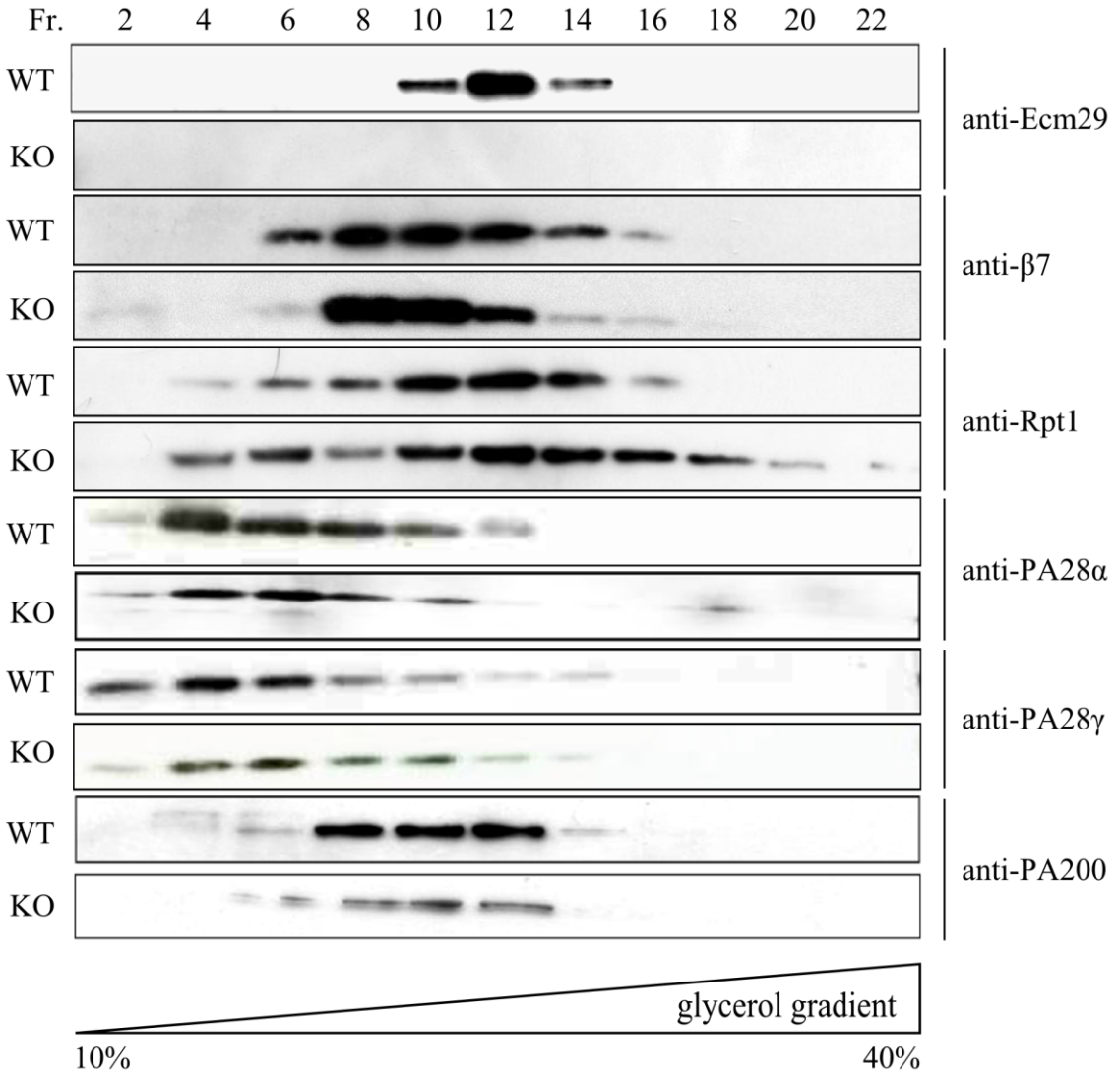

Figure 10 | Distributions of proteasome components on sedimentation gradient.

Distributions of Ecm29, CP subunit (β7) and proteasome activators (Rpt1, PA28α, PA28γ and PA200) on sedimentation velocity centrifugation. 1 mg of testis lysates were fractionated by glycerol density gradient centrifugation (10-40% glycerol from 1-22 fractions) and every two fractions were combined as one lane for immunoblot analyses. Antibodies used are indicated. WT; wild-type, KO; *KIAA0368*-deficient mice.

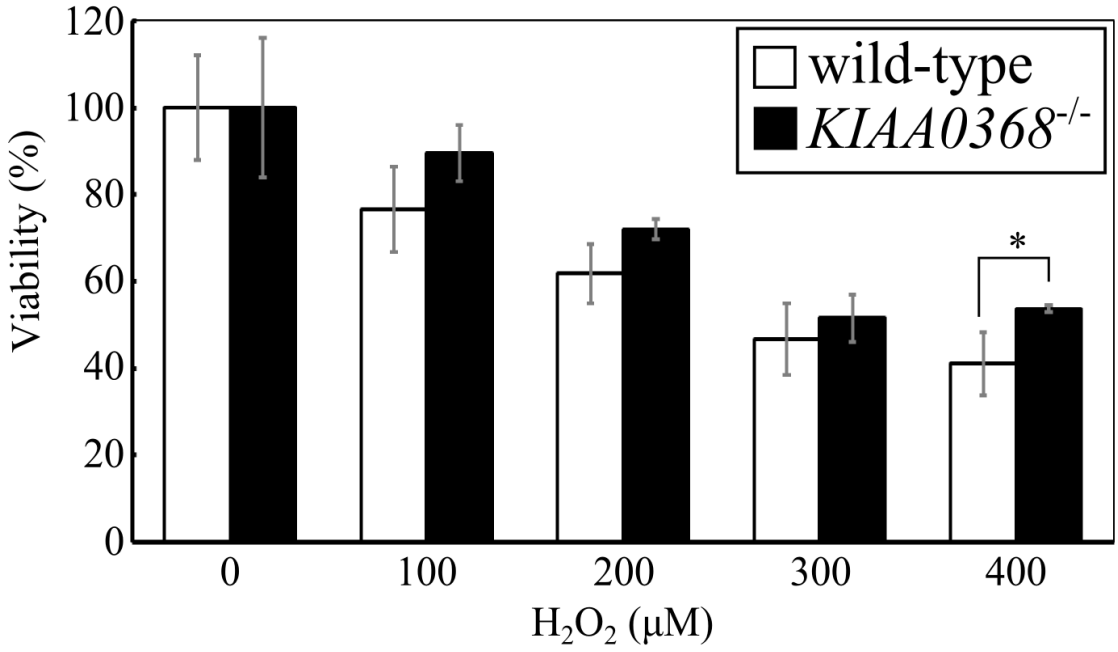

Figure 11 | Cell viabilities under oxidative stress.

Cell viability assay under oxidative stress. 3×10^3 cells were cultured in H_2O_2 of indicated concentrations and their viabilities were measured by WST assay. The bar charts represent the mean ± S.D. to untreated cells. White bars; wild-type, black bars; *KIAA0368*$^{-/-}$. *$P <$ 0.05 by student's *t*-test.

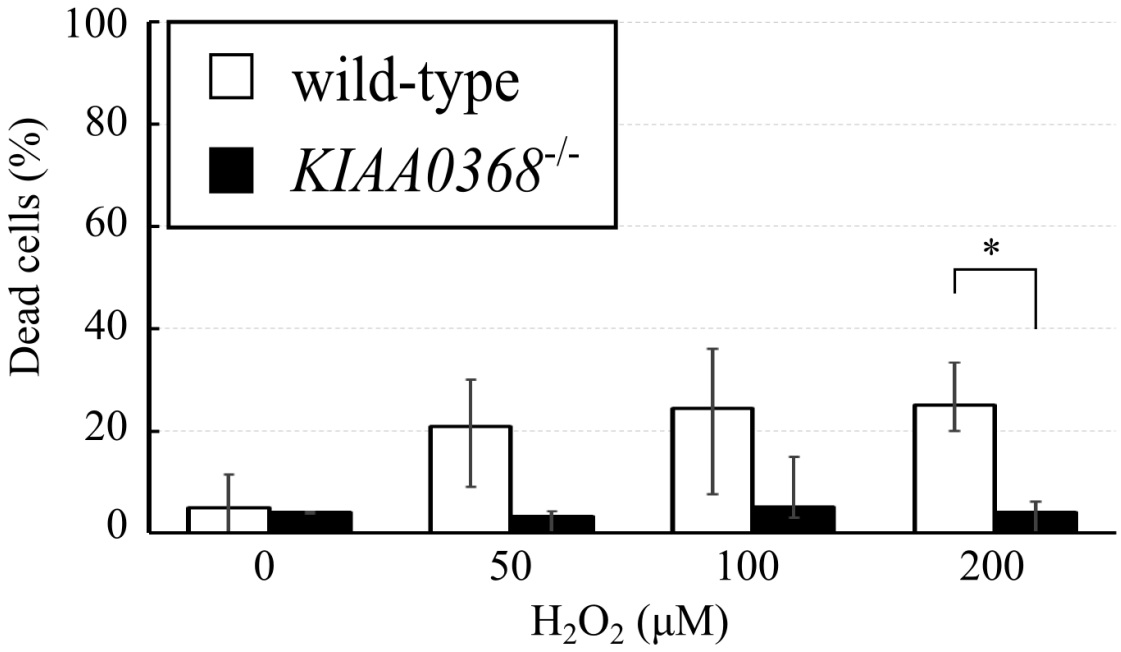

Figure 12 | Cell death under oxidative stress.

Trypan blue exclusion assay on oxidative stress. Wild-type and *KIAA0368*-deficient MEF cells were treated with indicated concentrations of H_2O_2 for 2 h. Dead cells were counted and the ratio of dead cells per total cells were calculated. The bar charts represent the mean ± S.D. White bars; wild-type, black bars; *KIAA0368*$^{-/-}$. *$P < 0.05$ by student's *t*-test.

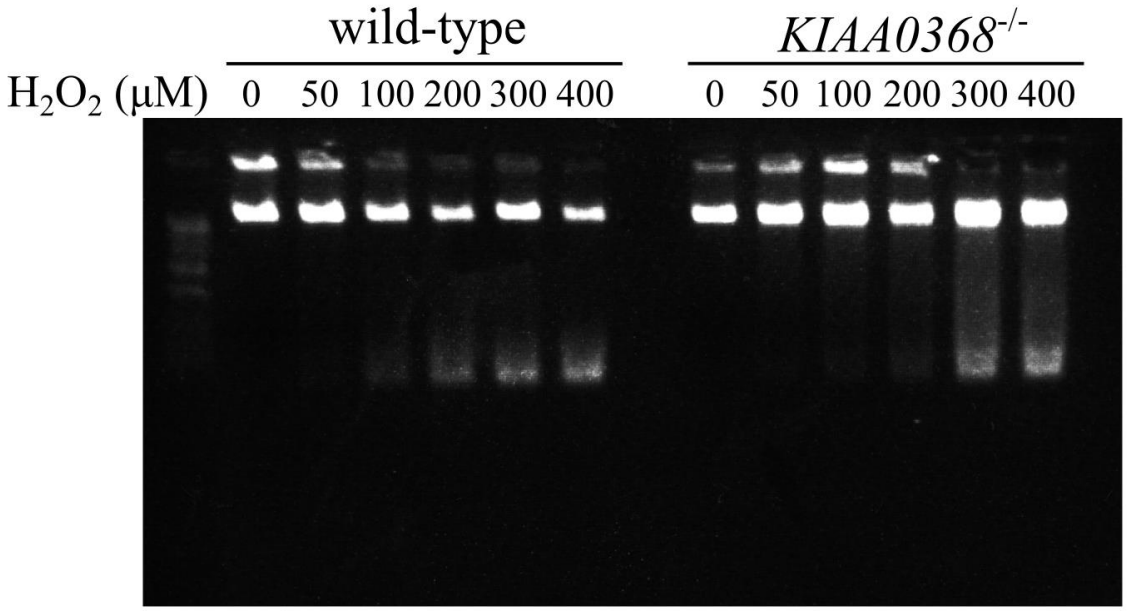

Figure 13 | Cell death-induced DNA fragmentations upon oxidative stress.

DNA ladder assay under oxidative stress. Wild-type and *KIAA0368*-deficient MEF cells were treated with indicated concentrations of H_2O_2 for 2 h. Genomic DNA were extracted and 0.5 μg of genomic DNA were electrophoresed on 1% agarose gel and visualized under UV illuminator.

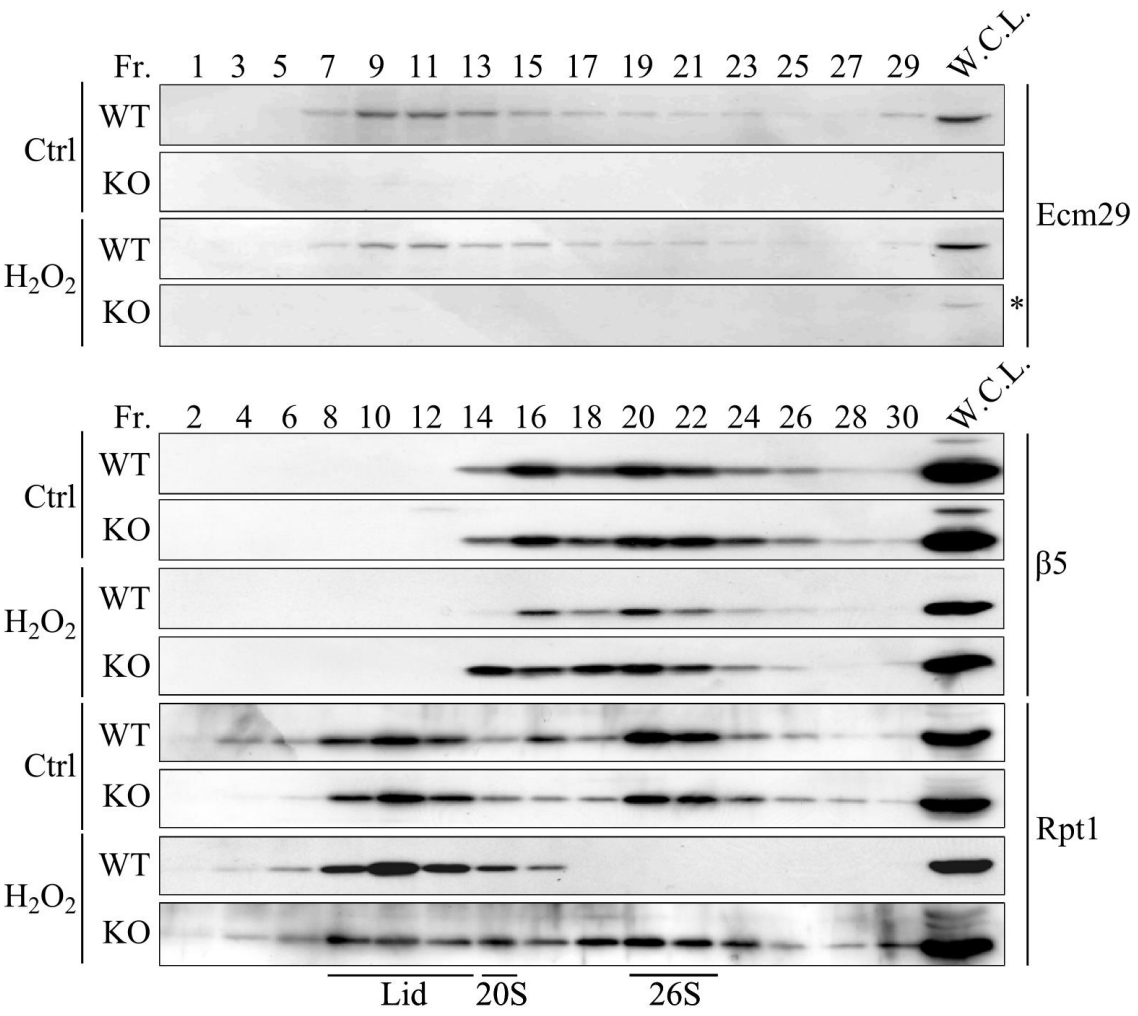

Figure 14 | Distrubutions of proteasome components under oxidative stress.

Analysis of proteasome complexes under oxidative stress. Wild-type (WT) or *KIAA0368*-deficient (KO) MEF cells were treated with 100 μM H_2O_2 or H_2O for 20 min. 500 μg of whole cell lysates were fractionated by glycerol density gradient (10-40% glycerol from 1-32 fractions) and immunoblotted with indicated antibodies. Asterisk indicates non-specific bands. W.C.L.; whole cell lysate.

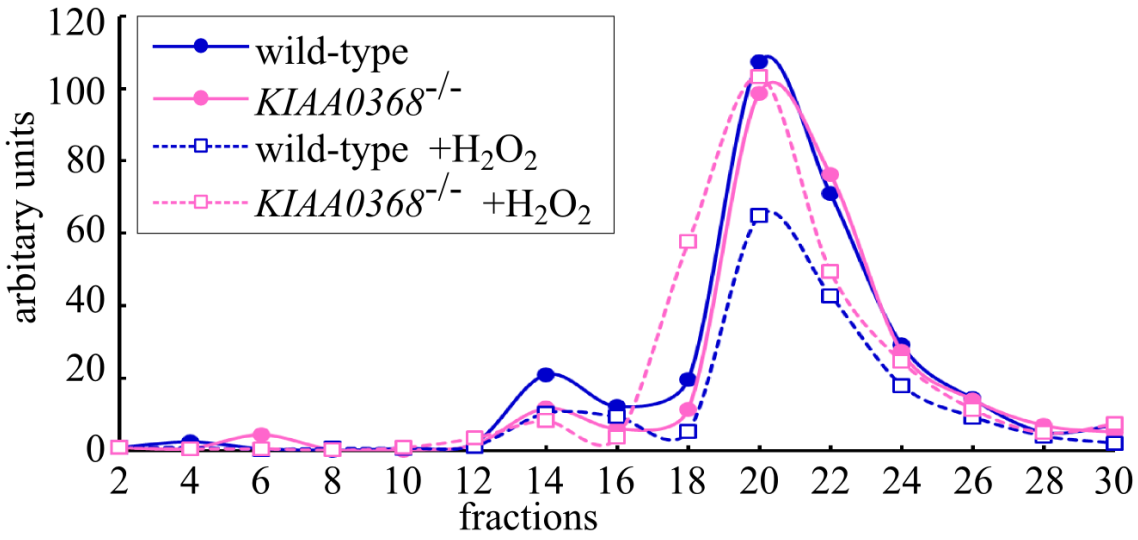

Figure 15 | Peptidase activities upon oxidative stress.

Peptidase activities under oxidative stress. Odd fractions prepared in (A) were measured using Suc-LLVY-AMC. The vertical axis represent relative fluorescence normalized to peptidase activity of the first fraction.

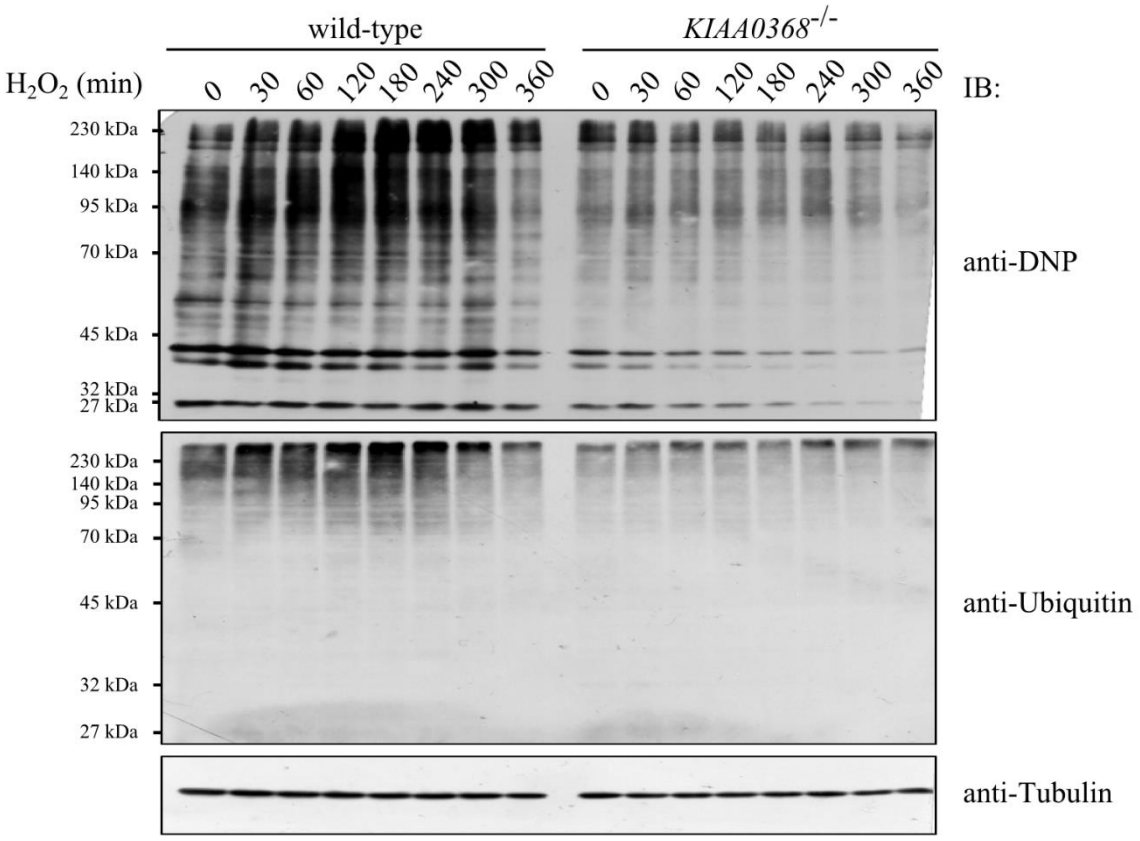

Figure 16 | Accumulation of oxidized and ubiquitylated proteins by H_2O_2 exposure. Detection of oxidatively damaged proteins. Wild-type and *KIAA0368*-deficient MEF cells were treated with 200 μM H_2O_2 for indicated times, then cell lysates were immunoblotted with indicated antibodies.

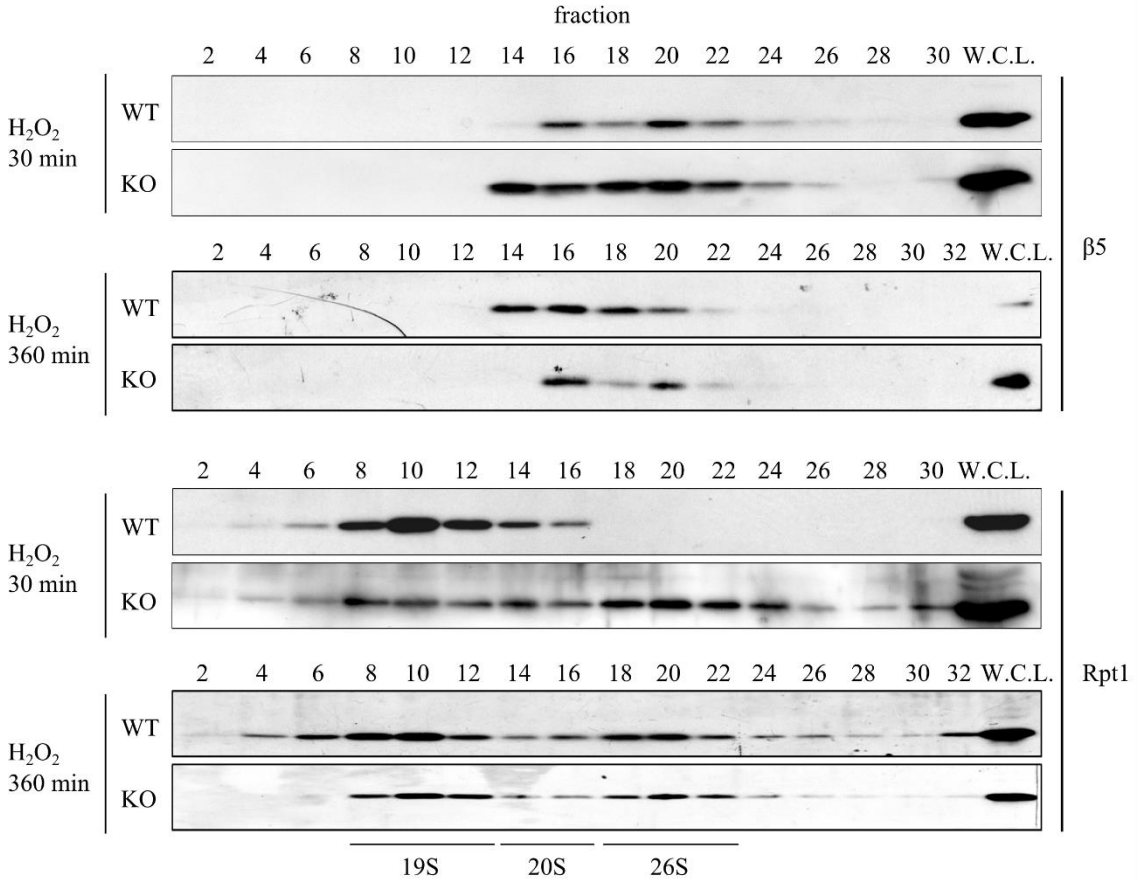

Figure 17 | Distribution of proteasome components after long-term H_2O_2 exposure. Analysis of proteasome complexes under oxidative stress. Wild-type (WT) or *KIAA0368*-deficient (KO) MEF cells were treated with 100 μM H_2O_2 for 30 min or 360 min. 500 μg of whole cell lysates were fractionated by glycerol density gradient (10-40% glycerol from 1-32 fractions) and immunoblotted with indicated antibodies. W.C.L.; whole cell lysate.

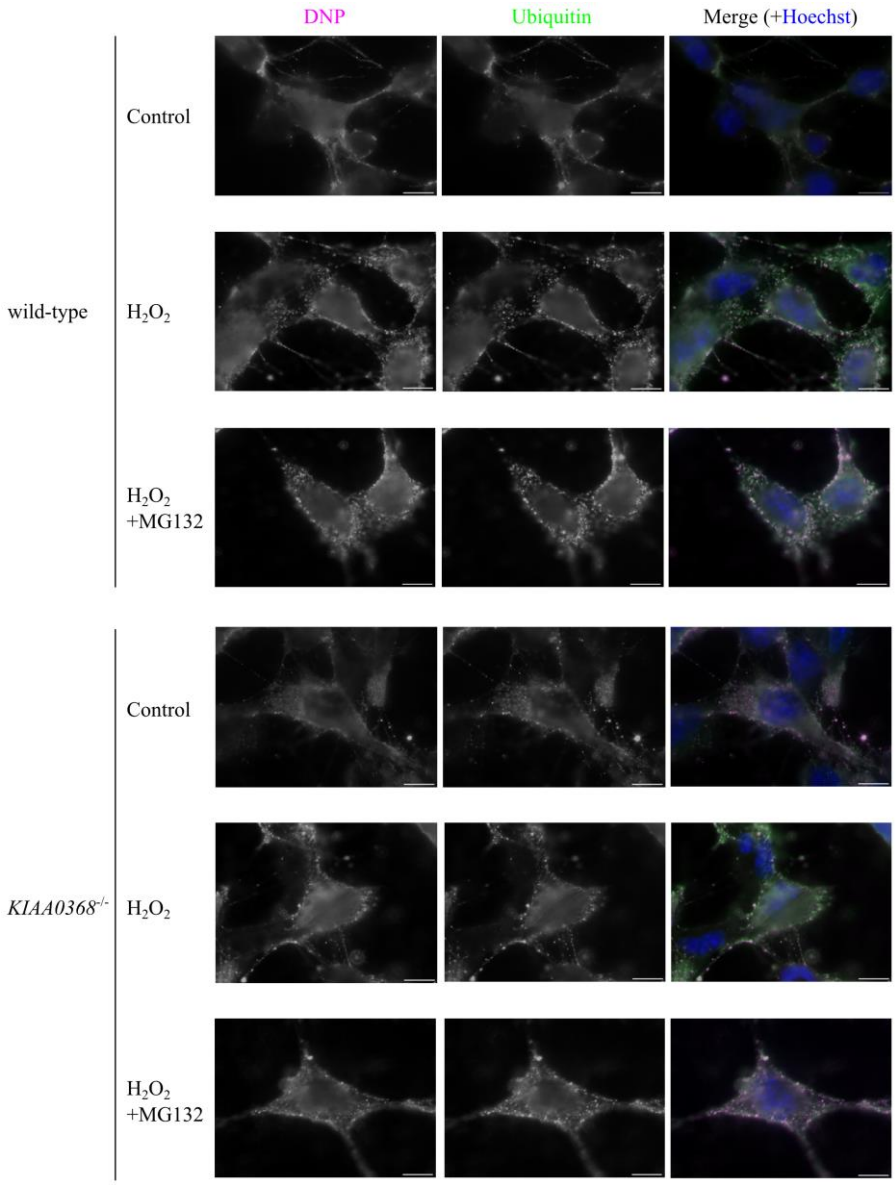

Figure 18 | Accumulation of carbonylated proteins in the cell.

Wild-type and *KIAA0368*$^{-/-}$ cells were treated with 200 μM H_2O_2 in the presence or absence of 20 μM MG132 and stained with indicated antibodies. Scale bars indicate 10 μm.

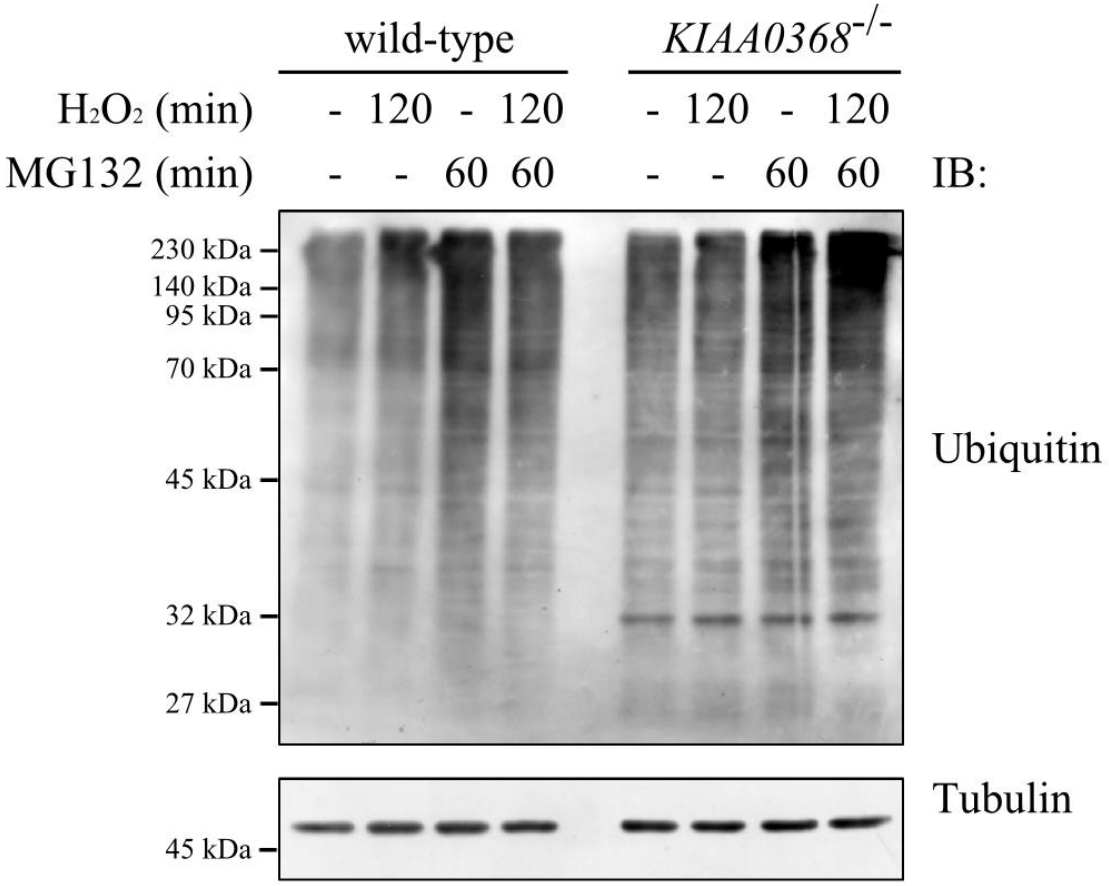

Figure 19 | Accumulation of ubiquitylated proteins in the presence of MG132.

Wild-type and *KIAA0368*-deficient MEF cells were treated with 200 μM H_2O_2 for 120 min in the presence or absence of 20 μM MG132 for 60 min, then cell lysates were immunoblotted with indicated antibodies.